Bipolar Resistive Switching Characteristics of Thermally Evaporated V_2O_5 Thin Films

Zhenni Wan, Hashem Mohammad, Yunqi Zhao, Robert Bruce Darling, and M. P. Anantram

***Abstract*— Forming-free bipolar resistive switching has been reported in ITO/V_2O_5/ITO structures. The sandwiched V_2O_5 film was synthesized by the sol–gel process, and it suffers from the issues of non-uniformity, low thermal stability, and short lifetime due to the presence of intercalated water molecules. In this work, thermal evaporation was employed for the deposition of amorphous V_2O_5 in ITO/V_2O_5/ITO structures. Bipolar resistive switching characteristics were preserved and insensitive to annealing temperature below 300 °C. Switching disappears when the annealing temperature exceeds 350 °C due to the re-crystallization of the amorphous film. Ab initio molecular dynamics method was utilized to simulate the melt-quench process and generate the amorphous V_2O_5 structure. Significantly, lowered formation energies were found at some oxygen vacancy sites in amorphous structure. The simulation was in agreement with the proposed switching mechanism that the generation of mobile oxygen ions in V_2O_5 film was essential for the occurrence of resistive switching. The lifetime and the compatibility with IC fabrication of the devices have also been greatly improved.**

***Index Terms*— ReRAMs, bipolar resistive switching, oxygen vacancies, vanadium pentoxide.**

I. Introduction

RESISTIVE switching random access memories (RRAMs) are widely considered as a promising candidate for the next-generation digital memory and neuromorphic computing [1]–[5]. Bipolar switching behavior has been reported in many oxides such as HfO_2 [6], [7], Ta_2O_5 [8], Al_2O_3 [9] and TiO_2 [10], where a conductive filament (CF) is formed which span across the oxide layer. The applied bias controls the drift and diffusion of oxygen ions and vacancies, therefore changing the resistance of the device by connecting and rupturing the CF under biases of opposite polarity [2]. Recently, a forming-free bipolar resistive switching behavior has been reported in ITO/V_2O_5/ITO structure where the switching occurs at the ITO/V_2O_5 interface instead of forming a CF [11]. It is proposed that in the interfacial V_2O_5 region, the migration of oxygen ions into and out of the top ITO electrode determines the low resistance state (LRS) and high resistance state (HRS) of the device.

In our previous study, the synthesized film from a sol-gel process is a xerogel phase with intercalated H_2O molecules, described by a chemical formula of $V_2O_5 \cdot nH_2O$ [12], [13]. The water content n decreases with increased annealing temperature, and intercalated water is fully evaporated from the film above 350°C. Reversible resistive switching only occurs with the presence of intercalated H_2O molecules. However, the film synthesized by the sol-gel process has poor uniformity, and its conductivity and switching voltages are sensitive to the annealing temperature due to variable water content in the film, making it incompatible with modern IC fabrication technology. Moreover, the device fabricated from the sol-gel process suffers from the issue of short lifetime due to the degradation of V_2O_5 thin film. The color usually transforms from orangish to greenish within one month, indicating a reduction of valence states from V^{5+} to V^{3+}/V^{4+}.

Manuscript received June 10, 2018; accepted July 7, 2018. Date of publication July 12, 2018; date of current version August 23, 2018. The review of this letter was arranged by Editor C. V. Mouli. *(Corresponding author: Zhenni Wan.)*

The authors are with the Department of Electrical Engineering, University of Washington, Seattle, WA 98195 USA (e-mail: jennywan@uw.edu).

Color versions of one or more of the figures in this letter are available online at http://ieeexplore.ieee.org.

Digital Object Identifier 10.1109/LED.2018.2855199

II. Methods

A. Fabrication and Measurement Setup

To overcome the downsides mentioned above for the sol-gel process, we have deposited V_2O_5 thin films by thermal evaporation and employed them in the ITO/V_2O_5/ITO structures in this work. ITO coated glass wafers with a sheet resistance of 20 Ω/sq were used as substrates and common bottom contacts. A thin film of V_2O_5 was then deposited by thermal evaporation in a vacuum deposition chamber. V_2O_5 powder was used as source material and evaporated from a tungsten boat. Note that the temperature of the boat was around 1,100°C during the deposition, which was above the melting point of V_2O_5 (690°C) but far below the melting point of other phases of vanadium oxide such as VO_2 (1,967°C) and V_2O_3 (1,940°C). Therefore, the great majority of the film was amorphous V_2O_5 and traces of other vanadium oxide should be negligible. The thickness of the deposited V_2O_5 thin film was measured by the built-in quartz crystal microbalance, and three different thicknesses were obtained: 11.4 nm, 23.5 nm and 53.0 nm. The as-fabricated V_2O_5 thin films are almost transparent with a slight yellowish color. XRD analysis was performed on the as-fabricated film and no significant peak was detected, indicating the amorphous nature of the film. The top ITO layer was deposited on top of the V_2O_5 thin film by magnetron sputtering. Two different ITO

0741-3106 © 2018 IEEE. Personal use is permitted, but republication/redistribution requires IEEE permission.
See http://www.ieee.org/publications_standards/publications/rights/index.html for more information.

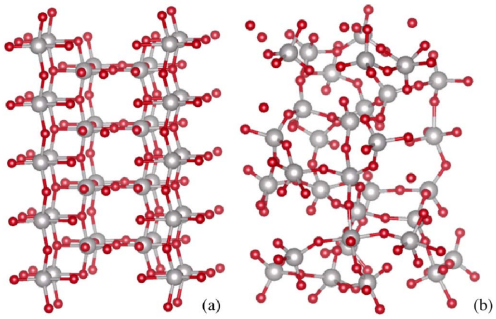


Fig. 1. Ball-and-stick models of the simulated (a) orthorhombic α-V_2O_5 (b) amorphous V_2O_5.

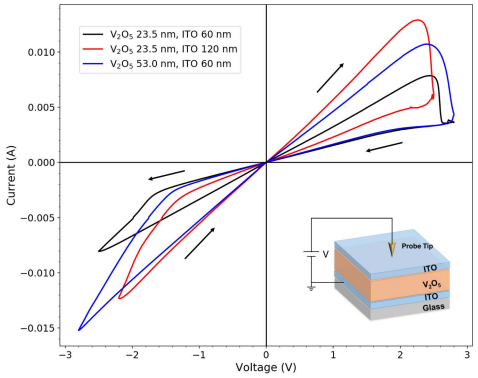


Fig. 2. I-V characteristics of as-fabricated devices. (Inset) Device structure and bias setup.

thicknesses were chosen: 60 nm and 120 nm. The fabricated ITO/V_2O_5/ITO device was then annealed in a box furnace in an ambient environment at temperatures ranging from 150°C to 375°C. The current-voltage characteristics of the devices were measured using a Keithley 4200 SCS parametric analyzer and a custom-built probe station.

B. Simulation

First-principle calculations of oxygen vacancy formation energies of both crystalline and amorphous V_2O_5 have been performed to obtain microscopic insights into our results. For all calculations, the spin polarized periodic DFT code Vienna Ab-initio Simulation Package (VASP) [14], [15] was employed, in which valence electronic states were described within a plane wave basis set with a cutoff energy of 520 eV. The core electrons were represented using projector augmented wave (PAW) pseudopotential [16]. Exchange–correlation energy was treated by using the Perdew-Burker-Ernzerhof [17] within the Generalized Gradient Approximation (GGA) method [18]. Rotationally invariant GGA+U [19] with a coulomb repulsion of $\mathbf{U} = 3.25$ eV was applied to the system [20]. Structural optimization was performed by relaxing the atoms using conjugate-gradient method [21].

In order to compare the present experiments with computations, amorphous V_2O_5 was modeled by the melt-quench process. Our modeling of amorphous V_2O_5 started from the corresponding crystalline material and used ab initio molecular dynamics simulations included in the VASP code. An orthorhombic α-V_2O_5 system consists of 112 atoms ($1 \times 4 \times 2$ supercell) was first fully melted at 2000 K with 18-ps-long time steps. Then the system was quenched from 2000 K to 300 K in 4000 more MD runs with 12-ps-long steps. After another 3-ps-long MD run at 300 K to stabilize the system, the last snapshot of this simulation was optimized at zero Kelvin to obtained to fully quenched amorphous state. The obtained amorphous structure is shown in Fig. 1.

III. Results

A. I-V Characteristics and Dependence on Annealing

The I-V characteristics of the as-fabricated devices are shown in Fig. 2, and the bias setup is shown in the inset. All of the devices exhibited bipolar switching characteristics before any post annealing process, except for the devices with 11.4 nm V_2O_5 layer (results no shown in the plot). The devices show LRS in their pristine states, and can be programmed to HRS under a positive bias of +2.5 V. A negative bias of −2.5 V can erase the programmed state and change the resistance back to LRS. The switching occurs at similar voltage levels for the three tested devices with different thickness of V_2O_5 and/or ITO layers. However, it is counter-intuitive that the current level increases with thickness of V_2O_5 and ITO layer. This behavior can be explained by the fact that top electrode (essentially the probe tip) and bottom electrode are asymmetrical in geometry and ITO is not a perfect metallic conductor that allows current to fully spread across its covered area. Although an increase in thickness enlarges the distance of the current path in vertical direction, it also supports more spreading of current in horizontal plane, giving rise to the overall increase in current.

It is observed that the device with 11.4 nm thick V_2O_5 layer does not show reversible switching behavior. Instead, an irreversible breakdown occurs at +2.5 V bias, resulting in partial ablation of the ITO film underneath the probe tip. The high electric field and current density generated in V_2O_5 thin film are likely to be the cause of such breakdown. The result suggests a lower limit for the thickness of V_2O_5 layer. Despite the difference in deposition method of V_2O_5 film, a similar programming/erasing speed of < 200 ns is expected as reported in [11]. Preliminary endurance cycling tests of the device have also been performed (results not listed). Degradation of ON/OFF ratios is observed after about 10 cycles. Further engineering of fabrication process is required to solve this issue.

In our previous study, V_2O_5 thin films synthesized by the sol-gel process suffers from dramatic changes in both atomic structure and electrical conductivity during the post annealing process due to the variable intercalated water content. To test the thermal stability of the ITO/V_2O_5/ITO structures fabricated by thermal evaporation, the same device (23.5 nm V_2O_5 and 60 nm ITO) was annealed at temperatures increasing from 200°C to 375°C, followed by I-V measurements after each annealing step. The results are shown in Fig. 3.

Compared to the as-fabricated state, the positive switching voltage increases by about 500 mV after a soft baking at 200°C, and a smaller increase is observed for negative

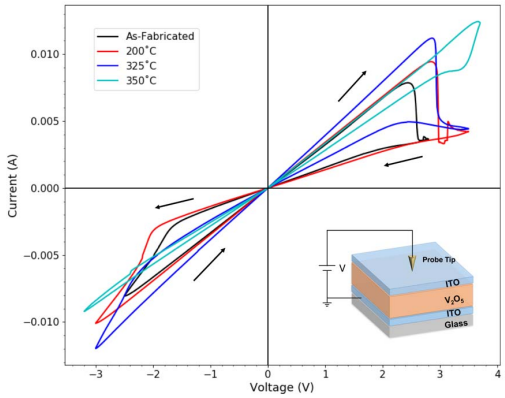


Fig. 3. Dependence of I-V characteristics on annealing temperatures.

switching voltage. The device then shows stable I-V characteristics up to annealing temperatures of 300°C. Further increase in annealing temperature to 325°C raises the current in both LRS and HRS, resulting in a degradation in ON/OFF ratio. At 350°C, the switching voltage increases up to +3.7 V and switching behavior is almost negligible. Bipolar switching fully disappears when the annealing temperature increases to 375°C. Overall the device exhibits much improved thermal stability over the devices fabricated using the sol-gel process.

The disappearance of bipolar switching characteristics at high annealing temperatures can be explained by the recrystallization of the amorphous V_2O_5 thin film. It has been reported [22] that amorphous V_2O_5 films deposited by thermal evaporation crystallize and transform to an orthorhombic phase when annealed in an oxygen rich environment at 400°C. ITO is a degenerate n-type semiconductor rich in oxygen vacancies, and its structure and electrical properties also changes dramatically with annealing temperature [23]. The annealing of ITO films in air will lead to the filling of oxygen vacancies due to their reaction with free oxygen. According to our proposed switching mechanism, the loss of oxygen vacancies in the ITO electrode can also result in the disappearance of resistive switching behavior. To rule out this possibility, a pre-annealing of amorphous V_2O_5 film at 400°C was performed in ambient air followed by deposition of the top ITO electrode by magnetron sputtering. No reversible switching was found in the as-fabricated devices, indicating that the transition of the amorphous V_2O_5 film into a crystalline phase is responsible for the disappearance of resistive switching.

B. Simulation of Oxygen Vacancy Formation Energies

Formation of oxygen vacancies in the V_2O_5 layer plays an important role in inducing the resistive switching behavior in ITO/V_2O_5/ITO structures. Ab initio calculations have been performed to investigate the formation energies of oxygen vacancies in amorphous V_2O_5 structures compared to the crystalline orthorhombic α-V_2O_5 phase.

The energy of vacancy formation energy was calculated according to the equation:

$$\Delta E^V_{form} = E^V - E^{prisine} + \frac{1}{2}\mu_{O_2},$$

TABLE I
OXYGEN VACANCY FORMATION ENERGIES IN AMORPHOUS V_2O_5

Vacancy Site	Formation Energy (eV)	Difference from α-V_2O_5 (eV)
O(1) a-V_2O_5	0.428	-1.222
O(2) a-V_2O_5	1.000	-0.650
O(3) a-V_2O_5	1.090	-0.560
O(4) a-V_2O_5	1.609	-0.041
O(5) a-V_2O_5	1.687	0.037
O(6) a-V_2O_5	1.892	0.242
O(7) a-V_2O_5	1.976	0.326
O(8) a-V_2O_5	2.090	0.440
O(9) a-V_2O_5	2.148	0.498

where E^V is the energy of the system with a vacancy, $E^{prisine}$ is the energy of the system without the vacancy, and μ_{O_2} is the chemical potential of molecular oxygen. In α-V_2O_5, the vacancy sites where the removed oxygen atom is bonded to a single vanadium atom has been taken into consideration as it has been reported to have the lowest formation energy [24]. The computed formation energy is 1.65 eV and it is used as a reference to evaluate how easily the amorphous structure can generate oxygen vacancies. Among the 80 oxygen atoms in the amorphous structure, nine were randomly picked and the calculated formation energies are listed in Table I.

We observe that, among the nine oxygen vacancy sites, three have significantly lower formation energies than the bulk case, which is to be expected given the metastability of the amorphous structure. Compared to the bulk form where all atoms tend to remain fixed in their original positions in the lattice after removing one oxygen, the atoms in the amorphous structure could experience more significant movements and thus result in a lower energy states. Two oxygen vacancy sites have similar formation energies and the remaining four sites have significantly higher formation energies. Therefore, these simulations show that it is easier to create oxygen vacancies in amorphous V_2O_5 than the orthorhombic bulk phase, which is consistent with our previous experimental observations.

IV. CONCLUSION

Our calculations have confirmed that the formation energies of oxygen vacancies can be lowered in the amorphous structure without the presence of intercalated H_2O molecules, which enables the reversible resistive switching in thermally evaporated ITO/V_2O_5/ITO devices. The removal of intercalated water also improves the lifetime of the devices. Excellent reversible switching characteristics are still preserved after seven months of exposure to air, compared to the one-month lifetime for the device fabricated from the sol-gel process.

REFERENCES

[1] R. Waser, R. Dittmann, G. Staikov, and K. Szot, "Redox-based resistive switching memories—Nanoionic mechanisms, prospects, and challenges," *Adv. Mater.*, vol. 21, pp. 2632–2663, Jul. 2009.

[2] H.-S. P. Wong, H.-Y. Lee, S. Yu, Y.-S. Chen, Y. Wu, P.-S. Chen, B. Lee, F. T. Chen, and M.-J. Tsai, "Metal-oxide RRAM," *Proc. IEEE*, vol. 100, no. 6, pp. 1951–1970, Jun. 2012.

[3] J. Cong and B. Xiao, "FPGA-RPI: A novel FPGA architecture with RRAM-based programmable interconnects," *IEEE Trans. Very Large Scale Integr. (VLSI) Syst.*, vol. 22, no. 4, pp. 864–877, Apr. 2014.

[4] M. D. Pickett, G. Medeiros-Ribeiro, and R. S. Williams, "A scalable neuristor built with Mott memristors," *Nature Mater.*, vol. 12, pp. 114–117, Dec. 2012.

[5] S. Yu, B. Gao, Z. Fang, H. Yu, J. Kang, and H.-S. P. Wong, "A low energy oxide-based electronic synaptic device for neuromorphic visual systems with tolerance to device variation," *Adv. Mater.*, vol. 25, pp. 1774–1779, Mar. 2013.

[6] H. Y. Lee, P. S. Chen, T. Y. Wu, Y. S. Chen, C. C. Wang, P. J. Tzeng, C. H. Lin, F. Chen, C. H. Lien, and M.-J. Tsai, "Low power and high speed bipolar switching with a thin reactive Ti buffer layer in robust HfO_2 based RRAM," in *IEDM Tech. Dig.*, Dec. 2008, pp. 1–4.

[7] Y. Wang, Q. Liu, S. Long, W. Wang, Q. Wang, M. Zhang, S. Zhang, Y. Li, Q. Zuo, J. Yang, and M. Liu, "Investigation of resistive switching in Cu-doped HfO_2 thin film for multilevel non-volatile memory applications," *Nanotechnology*, vol. 21, no. 4, p. 045202, 2010.

[8] D. S. Jeong, R. Thomas, R. S. Katiyar, J. F. Scott, H. Kohlstedt, A. Petraru, and C. S. Hwang, "Emerging memories: Resistive switching mechanisms and current status," *Rep. Prog. Phys.*, vol. 75, no. 7, p. 076502, 2012.

[9] C.-Y. Lin, C.-Y. Wu, C.-Y. Wu, C. Hu, and T.-Y. Tseng, "Bistable resistive switching in Al_2O_3 memory thin films," *J. Electrochem. Soc.*, vol. 154, no. 9, pp. G189–G192, 2007.

[10] D. S. Jeong, H. Schroeder, and R. Waser, "Coexistence of bipolar and unipolar resistive switching behaviors in a $Pt/TiO_2/Pt$ stack," *Electrochem. Solid-State Lett.*, vol. 10, no. 8, pp. G51–G53, 2007.

[11] Z. Wan, R. B. Darling, A. Majumdar, and M. P. Anantram, "A forming-free bipolar resistive switching behavior based on $ITO/V_2O_5/ITO$ structure," *Appl. Phys. Lett.*, vol. 111, no. 4, p. 041601, 2017.

[12] V. Petkov, P. N. Trikalitis, E. S. Bozin, S. J. L. Billinge, T. Vogt, and M. G. Kanatzidis, "Structure of $V_2O_5{\cdot}nH_2O$ xerogel solved by the atomic pair distribution function technique," *J. Amer. Chem. Soc.*, vol. 124, no. 34, pp. 10157–10162, 2002.

[13] Z. Wan, R. B. Darling, and M. P. Anantram, "Programmable diode/resistor-like behavior of nanostructured vanadium pentoxide xerogel thin film," *Phys. Chem. Chem. Phys.*, vol. 17, no. 45, pp. 30248–30254, 2015.

[14] G. Kresse and J. Hafner, "*Ab initio* molecular-dynamics simulation of the liquid-metal–amorphous-semiconductor transition in germanium," *Phys. Rev. B, Condens. Matter*, vol. 49, pp. 14251–14269, May 1994.

[15] G. Kresse and J. Furthmüller, "Efficient iterative schemes for *ab initio* total-energy calculations using a plane-wave basis set," *Phys. Rev. B, Condens. Matter*, vol. 54, pp. 11169–11186, Oct. 1996.

[16] P. E. Blöchl, "Projector augmented-wave method," *Phys. Rev. B, Condens. Matter*, vol. 50, pp. 17953–17979, Dec. 1994.

[17] J. P. Perdew, K. Burke, and M. Ernzerhof, "Generalized gradient approximation made simple," *Phys. Rev. Lett.*, vol. 77, pp. 3865–3868, Oct. 1996.

[18] J. P. Perdew, J. A. Chevary, S. H. Vosko, K. A. Jackson, M. R. Pederson, D. J. Singh, and C. Fiolhais, "Atoms, molecules, solids, and surfaces: Applications of the generalized gradient approximation for exchange and correlation," *Phys. Rev. B, Condens. Matter*, vol. 46, no. 11, pp. 6671–6687, 1992.

[19] A. I. Liechtenstein, V. I. Anisimov, and J. Zaanen, "Density-functional theory and strong interactions: Orbital ordering in Mott-Hubbard insulators," *Phys. Rev. B, Condens. Matter*, vol. 52, pp. R5467–R5470, Aug. 1995.

[20] L. Wang, T. Maxisch, and G. Ceder, "Oxidation energies of transition metal oxides within the GGA+U framework," *Phys. Rev. B, Condens. Matter*, vol. 73, p. 195107, May 2006.

[21] W. H. Press, *Numerical Recipes: The Art of Scientific Computing*, 3rd ed. New York, NY, USA: Cambridge Univ. Press, 1986.

[22] R. Santos, J. Loureiro, A. Nogueira, E. Elangovan, J. V. Pinto, J. P. Veiga, T. Busani, E. Fortunato, R. Martins, and I. Ferreira, "Thermoelectric properties of V_2O_5 thin films deposited by thermal evaporation," *Appl. Surf. Sci.*, vol. 282, pp. 590–594, Oct. 2013.

[23] Y. Hu, X. Diao, C. Wang, W. Hao, and T. Wang, "Effects of heat treatment on properties of ITO films prepared by RF magnetron sputtering," *Vacuum*, vol. 75, no. 2, pp. 183–188, 2004.

[24] D. O. Scanlon, A. Walsh, B. J. Morgan, and G. W. Watson, "An ab initio study of reduction of V_2O_5 through the formation of oxygen vacancies and Li intercalation," *J. Phys. Chem. C*, vol. 112, pp. 9903–9911, Jun. 2008.